Ramsauer-Townsend effect in muonic atom scattering

F. Mulhauser,[1,*] A. Adamczak,[2,†] G. A. Beer,[3] V. M. Bystritsky,[4] M. Filipowicz,[5] M. C. Fujiwara,[6] T. M. Huber,[7] O. Huot,[1]
R. Jacot-Guillarmod,[1,‡] P. Kammel,[8,*] S. K. Kim,[9] P. E. Knowles,[1] A. R. Kunselman,[10] G. M. Marshall,[6] A. Olin,[6]
C. Petitjean,[11] T. A. Porcelli,[6] L. A. Schaller,[1] V. A. Stolupin,[4] J. Woźniak,[12] and J. Zmeskal[13]

(TRIUMF Muonic Hydrogen Collaboration)

[1]*Department of Physics, University of Fribourg, CH-1700 Fribourg, Switzerland*
[2]*Henryk Niewodniczański Institute of Nuclear Physics, Polish Academy of Sciences, PL-31342 Cracow, Poland*
[3]*Department of Physics and Astronomy, University of Victoria, Victoria, Canada, V8W 2Y2*
[4]*Laboratory of Nuclear Problems, Joint Institute for Nuclear Research, Dubna 141980, Russia*
[5]*Faculty of Fuels and Energy, AGH University of Science and Technology, PL-30059 Krakow, Poland*
[6]*TRIUMF, Vancouver, Canada, V6T 2A3*
[7]*Gustavus Adolphus College, St. Peter, Minnesota 56082, USA*
[8]*University of California, Berkeley, California 94720, USA*
[9]*Physics Department, Jeonbuk National University, Jeonju, Jeonbuk 561-756, S. Korea*
[10]*University of Wyoming Physics, Laramie, Wyoming 82071-3905, USA*
[11]*Paul Scherrer Institute, CH-5232 Villigen PSI, Switzerland*
[12]*Faculty of Physics and Applied Computer Science, AGH University of Science and Technology, PL-30059 Krakow, Poland*
[13]*Stefan Meyer Institut für Subatomare Physik, Austrian Academy of Sciences, A-1090 Wien, Austria*

We present the final results of an experimental study of μd and μt atom scattering in solid hydrogen cooled to 3 K. Strong effects resulting from the Ramsauer-Townsend effect have been observed in the TRIUMF experiment E742 where muons were stopped in thin frozen layers of hydrogen. The measured Ramsauer-Townsend minimum energy for both μd and μt atoms and the minimum cross section are in agreement with theory.

Negative muons stopping in hydrogen can form muonic hydrogen (μh) atoms, where $h=p, d$, or t depending on the hydrogen isotope. Although created in excited states, such atoms cascade to the ground state quickly (10^{-9} s), where their kinetic energy is of the order of several eV, much higher than thermal equilibrium energies. The muonic hydrogen atom is about 200 times smaller (m_μ/m_e scaling) than the size of ordinary electronic hydrogen. The small neutral atom can easily diffuse through the surrounding medium, undergoing different types of interactions with atoms and molecules including elastic and inelastic scattering.

The scattering processes

$$\mu d + H_2 \rightarrow \mu d + H_2$$

and

$$\mu t + H_2 \rightarrow \mu t + H_2 \tag{1}$$

are predicted [1–4] to show a dramatic minimum in scattering, the so-called Ramsauer-Townsend (RT) effect. This effect is due to a minimum scattering cross section ($\sim 10^{-21}$ cm^2) at collision energies between 2 and 30 eV.

These cross sections are more than two orders of magnitude smaller than the $\mu p + H_2$ one [5]. The result is a quasitransparency of the H_2 molecules for incident μd or μt atoms. Theoretical calculations for muonic atoms scattering in solid or gas are performed in Refs. [4–7]. However, the improvements in those calculations are important for muonic atoms of low energy and negligible for energies above eV [5].

The development at TRIUMF of multilayer thin frozen hydrogen film targets [8–14], which produce muonic atom beams emitted into vacuum, permitted the cross sections to be probed in an interesting way. We have studied several isolated muon induced processes using a time-of-flight (TOF) method developed by the frozen target geometry [14].

The aim of the present experiment was to study and verify the cross sections in the RT minimum of μd and μt elastic scattering in solid hydrogen. The experiments were performed at the M20B muon channel at TRIUMF. The layout of the apparatus was shown and described in Refs. [5,15–17]. Gaseous hydrogen (or neon) was sprayed, using a special diffusion system, onto a 51 μm thick gold foil, kept at 3 K, where it froze creating thin solid films which could be maintained in high vacuum. Details of the target construction and working procedure are given in Refs. [9,18].

The muons eventually stop either in the gold target support foil or in the 800 μm thick solid hydrogen target where they finally form muonic atoms. The hydrogen target frozen on that foil, which is placed perpendicularly to the muon beam axis, is called the upstream target (US), and is made of pure protium or of protium with a small admixture of deuterium or tritium, depending on the experiment.

---

*Present address: University of Illinois at Urbana-Champaign, Urbana, Illinois 61801, USA.

†Also at Rzeszow University of Technology, PL-35959 Rzeszow, Poland.

‡Present address: Nordostlich Krafwerke, Switzerland.
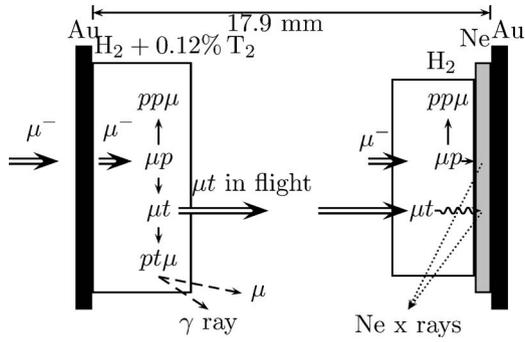
FIG. 1. Target scheme for μt. Muonic tritium atoms are emitted forward into the vacuum gap. The $pt\mu$ fusion emission is measured via the NaI(Tl) and scintillator detectors. The neon x rays are detected with two germanium detectors.

When deuterium or tritium was present in the US target, we used an additional downstream pure protium target (DS) frozen on a second gold foil placed parallel to the first foil but 17.9 mm further along the beam axis. Such an arrangement is presented in Fig. 1, where a thin layer of neon is shown sandwiched between a layer of pure protium and the DS gold foil, as used in the μt scattering experiment. A low muon beam momentum was chosen to minimize the number of μ^- stops in the DS protium layer [15], so that the muon stopped mainly in the US gold foil and hydrogen target layers.

Neon was used to detect the scattered muonic μt atoms which left the DS hydrogen layer and subsequently transferred the muon to the neon. The resulting emission of 207 keV x rays from the $2p$-$1s$ μNe transition was observed by two ~ 100 cm^3 germanium crystals with a time resolution of 10–12 ns, full width at half maximum. Plastic scintillators were located around the target to detect the muon decay electrons.

The US target was composed of protium with a small concentration of D_2 (or T_2), which served as a source of energetic μd (μt) atoms emitted from the layer into the adjacent vacuum with a mean energy of 3.5 eV (9 eV in the case of the H_2/T_2 mixture) as a result of the RT effect. In most cases (70–75 %) the muon was transferred from μp to a deuteron or triton, forming μd or μt atoms, respectively. At formation, the muonic deuterium (tritium) atoms had a relatively high kinetic energy, about 45 eV, which they subsequently lost in elastic collisions, mainly with protium, until the energy reached the range of the RT minimum in the scattering cross section $\sigma(\mu d + H_2)$. Then the mean distance between collisions increased and the hydrogen layer became effectively transparent for the μd and μt atoms which were then easily emitted from the solid into the adjacent vacuum. Such energetic emitted muonic atoms traveled through vacuum toward the downstream hydrogen layer (DS), and a fraction passed, after possible interactions in hydrogen, to the Ne layer, where it produced Ne x rays as a result of the muon transfer to neon and subsequent muonic neon deexcitation. Such μd (μt) atoms gave a characteristic peak in the TOF spectrum at ≈ 1 μs—a time determined by the distance between the foils and the energy of the RT minimum within the energy collision scale of μd (μt) atoms with H_2 molecules.

TABLE I. Measurements performed for the RT study. DE (deuterium emission) stands for a layer of 1500 Torr ℓ($H_2 + 0.05\% D_2$) covered with 500 Torr ℓ H_2. TE (tritium emission)— 2000 Torr ℓ($H_2 + 0.12\% T_2$). STE (small tritium emission)— 1000 Torr ℓ($H_2 + 0.12\% T_2$). GMU—good muons: i.e., events when only one muon entered the apparatus (no pileup). Conversion factor (for hydrogen): 1 Torr ℓ corresponds to 3.4 μg cm^{-2} for H_2 [19]. Beam momentum was 26.70 MeV/c and 26.25 MeV/c for the deuterium and tritium, respectively.

Label	US Torr ℓ	DS protium Torr ℓ	DS Neon Torr ℓ	GMU$\times 10^6$
D1-D2	DE		100–50	510.2
D3	DE	300	50	521.8
D4	DE	600	50	433.2
T1-T2	TE		30–50	287.7
T3	TE	350	50	405.3
T4	STE	500	50	147.1

Clearly, not all muons were stopped in the US target. Those which reached the second foil created μp's in the DS protium. The μp's diffused to neon giving a contribution to the time spectrum at early times. Thus the resulting Ne time spectrum contained two relatively distinct components, one of them connected with the RT effect in μd (μt) scattering and the other with the diffusion of μp atoms in the solid hydrogen. The full study of μp atom diffusion is given by Woźniak *et al.* [5].

Analyzing the time distribution of the μd's and μt's via the $2p$-$1s$ μNe transition gives information about the scattering cross sections. Table I summarizes the different measurements performed for the study of the RT effect. The last tritium measurement (T4) was not taken into account in previous publications [15,20], due to a different emission target. The essential part of the analysis is the comparison of the experimental time distributions with the ones calculated by Monte Carlo. The Monte Carlo code FOW [21] was used in the planning stages of the experiment as well as for the analysis to simulate all physical processes occurring after muons pass through the entrance window of the apparatus. Muon stopping distributions along the beam axis in the different apparatus components, especially in the hydrogen layers of the target, have been taken from a special set of measurements [15] and from another Monte Carlo calculation [22]. They are used as an input to FOW. Details about the method have already been given by Woźniak *et al.* [5].

Muonic atom scattering in hydrogen was measured via the x-ray time spectra of the μNe $2p$-$1s$ transition at 207 keV. The time spectra events were selected within an energy window between 205.6 and 208.3 keV. The background time spectra underneath the 207 keV peak were created using time spectra from two neighboring energy windows, namely a left background between 203.3 and 205.6 keV and a right background between 208.3 and 210.2 keV.

Two different background evaluation procedures were used. In the first, the left and right spectra were added, then normalized by the energy window widths, and the resulting spectrum was subtracted from the time spectrum of the
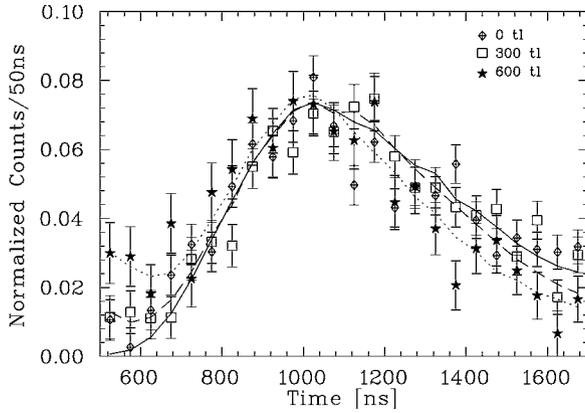
FIG. 2. Experimental TOF spectra (points with error bars) for the deuterium measurements. The solid, dashed, and dotted lines are the Monte Carlo (MC) simulations for D1-D2, D3, and D4, respectively.

μNe $2p$-$1s$ peak. The second method relied on a multiparameter fit of the summed left and right backgrounds using two exponential functions (with lifetimes for muons in gold and neon), and the background predicted from the fit function was then subtracted from the μNe $2p$-$1s$ peak. Since the background accounts for 70–85 % of the total statistics, its removal plays an important role, especially for data at early times where there is a strong contribution from the prompt muon capture in both the neon layer and the gold foils.

Another data cleaning method resulting in a considerably better signal to background ratio was the requirement that the muon decay electron be seen *after* the μNe $2p$-$1s$ x ray. Those electrons were detected by the scintillators during a time interval 0.2–5.2 μs after the μNe signal. This method, called the del$_e$ condition, suppressed the background by a factor of about 300. However, useful statistics were reduced by about a factor 10. Figures 2 and 3 show background subtracted TOF spectra for the μd and μt atom scattering, respectively, without the del$_e$ condition in all measurements. In the μt atom scattering experiment, due to a higher RT minimum energy, a distinction between μt and μp processes is more difficult to perform, as shown in Fig. 16 of Woźniak *et al.* [5].
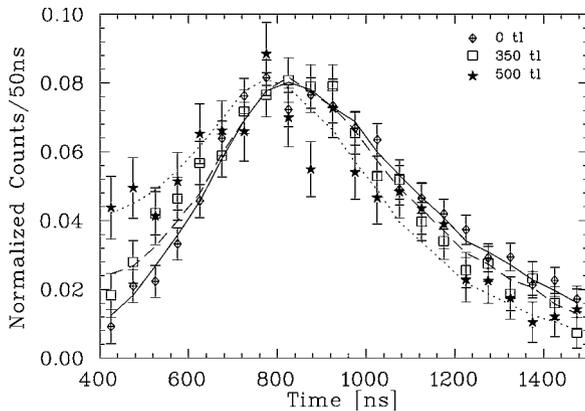
FIG. 3. Experimental TOF spectra (points with error bars) for the tritium measurements. The solid, dashed, and dotted lines are the MC simulations for T1-T2, T3, and T4, respectively.

TABLE II. Characteristic values used in the cross section parametrization for both μd and μt scattering. Energies are in the center of mass system (CMS) and cross sections [3] are given per one atom, i.e., for $\mu h + p \rightarrow \mu h + p$ processes.

Parameter	μd	μt	Units
E_R	1.7	3.0	eV
E_{min}	1	1	meV
E_{max}	190.5	51.3	eV
$\sigma(E_R)$	1.13	1.66	$\times 10^{-21}$ cm^2

A χ^2 analysis has been performed to fit the FOW input parameters to the experimental data. The theoretical cross sections $\sigma(\mu d + H_2)$ and $\sigma(\mu t + H_2)$ are varied in two different ways. We determine the position of the zero of the S-wave amplitude and the P-wave cross section at the RT minimum by introducing an energy shift ΔE and a depth factor df.

In contrast to previously published results [15] where the analysis consisted in varying only one parameter at a time, this final work was performed where both parameters ΔE and df were varied at the same time. The energy shift ΔE is obtained by transforming the energy axis according to $E \rightarrow E_{tr}$ and then $\sigma(E) \rightarrow \sigma(E_{tr})$. The energy transformations are

$$E_{tr} = \begin{cases} E + \dfrac{E - E_{min}}{E_R - E_{min}} \times \Delta E, & \text{for } E \leq E_R \\[2ex] E + \dfrac{E_{max} - E}{E_{max} - E_R} \times \Delta E, & \text{for } E > E_R \end{cases}, \qquad (2)$$

where E is the energy value before shifting and E_R the original value of the RT energy minimum. E_{min} and E_{max} are the minimum and maximum energy, corresponding to the left and right borders of the energy range. For $E = E_R$, the transformed energy E_{tr} given by Eq. (2) becomes $E_{tr} = E + \Delta E$. $\sigma(E_R)$ is the minimum cross section for the RT energy. Thus, this parametrization can be treated as a shift and the initial parameters are found in Table II.

The depth factor df is determined via a rescaled minimum cross section without changing the position of the minimum energy E_R,

$$\sigma_{exp}(E_R) = df \times \sigma(E_R). \qquad (3)$$

The rescaling took place in the CM energy range 0.5–10 eV. To preserve the smooth form of the cross sections, values within this energy range were not globally scaled by the factor df, but were scaled by a factor which ranged from 1 at the borders to the factor df at the RT minimum energy.

A spline interpolation was performed between the two-dimensional grid of the Monte Carlo simulation to fit the experimental data [23]. The fit starting time has been set to $t_{min} = 500$ (400) ns for μd (μt) atoms to avoid using the μp diffusion part [5] of the spectra in the analysis. The fit stopping time was chosen at $t_{max} = 1700$ (1500) ns for μd (μt) to avoid taking into account channels with extremely low statistics, where background subtraction plays a strong role. The

TABLE III. Results of the two-parameter analysis for the μd and μt atom scattering when data are combined. Errors contain the combination of statistical and systematics uncertainties.

Label	Depth factor df	Energy shift ΔE (eV)
D1-D4	1.10 ± 0.18	0.17 ± 0.13
T1-T4	1.22 ± 0.11	-0.25 ± 0.23

t_{max} time was varied in the present analysis by ± 200 ns, without any major effect on the fit results. Strong variations were seen in both the depth factor as well as the energy shift. Depending on the background subtraction method, the individual detector, as well as the fit interval, results scattered excessively. Variations up to 40% were obtained for both parameters. These variations were seen for both μd and μt measurements. As already seen in previously published works [15,20], the scattered results show that the two-parameter fit is not sufficiently constrained.

Therefore, we adopted a third approach, where all μd or μt data were fitted together. The starting and stopping times, as well as grid size, and minimization procedures, were all similar to the previous method. The new approach, namely that for each muonic atom type the energy shift and depth factors were required to simultaneously satisfy the best fit conditon for all three DS protium thickness, provides a strong constraint of the parameters and leads to the results given in Table III. Background subtraction, individual detectors, and fit intervals are taken into account for the systematic uncertainties which are still dominant.

The agreement between experiments and theory is good for μd and μt atom scattering. Both theoretical minimum RT energies, $E_R(\mu t) = 3.0$ eV and $E_R(\mu d) = 1.7$ eV, are compatible with our measurements. However, the RT determined cross section scaling factors suggest that the RT minima have a slightly shallower depth than theoretically predicted, particularly for μt atoms.

In conclusion, we have been able to measure the Ramsauer-Townsend cross sections for μd and μt atom scattering with a precision of 10–20 %. More sophisticated measurements with much better statistics are needed to improve these results.

[1] M. Bubak and M. P. Faifman, JINR Preprint E4-87-464 (1987).
[2] L. Bracci *et al.*, Muon Catal. Fusion **4**, 247 (1989).
[3] C. Chiccoli *et al.*, Muon Catal. Fusion **7**, 87 (1992).
[4] A. Adamczak *et al.*, At. Data Nucl. Data Tables **62**, 255 (1996).
[5] J. Woźniak *et al.*, Phys. Rev. A **68**, 062502 (2003).
[6] A. Adamczak, Hyperfine Interact. **119**, 23 (1999).
[7] A. Adamczak, Ph.D. thesis, Institute of Nuclear Physics, Kraków, Poland (2003) (unpublished).
[8] G. M. Marshall *et al.*, Hyperfine Interact. **82**, 529 (1993).
[9] P. E. Knowles *et al.*, Nucl. Instrum. Methods Phys. Res. A **368**, 604 (1996).
[10] F. Mulhauser *et al.*, Phys. Rev. A **53**, 3069 (1996).
[11] P. E. Knowles *et al.*, Phys. Rev. A **56**, 1970 (1997); **57**, 3136(E) (1998).
[12] M. C. Fujiwara *et al.*, Phys. Rev. Lett. **85**, 1642 (2000).
[13] T. A. Porcelli *et al.*, Phys. Rev. Lett. **86**, 3763 (2001).
[14] G. M. Marshall *et al.*, Hyperfine Interact. **138**, 203 (2001).
[15] F. Mulhauser *et al.*, Hyperfine Interact. **119**, 35 (1999).
[16] J. Woźniak *et al.*, Hyperfine Interact. **119**, 63 (1999).
[17] V. M. Bystritsky *et al.*, Hyperfine Interact. **138**, 47 (2001).
[18] G. M. Marshall *et al.*, Hyperfine Interact. **101/102**, 47 (1996).
[19] M. C. Fujiwara *et al.*, Nucl. Instrum. Methods Phys. Res. A **395**, 159 (1997).
[20] F. Mulhauser *et al.*, Hyperfine Interact. **138**, 41 (2001).
[21] J. Woźniak, V. M. Bystritsky, R. Jacot-Guillarmod, and F. Mulhauser, Hyperfine Interact. **101/102**, 573 (1996).
[22] R. Jacot-Guillarmod, *Stopping Code* (University of Fribourg, 1997).
[23] M. Filipowicz, V. M. Bystritsky, P. E. Knowles, F. Mulhauser, and J. Woźniak, Nucl. Instrum. Methods Phys. Res. A **547**, 652 (2005).